Incidence angle and spectral effects on vertical junction silicon solar cell capacitance

Moustapha SANE[1], **Gökhan ŞAHİN**[1], **Fabé Idrissa BARRO**[1,*],
Amadou Seidou MAIGA[2]

[1]Semiconductors and Solar Energy Laboratory, Faculty of Science and Technology,
Cheikh Anta Diop Universtity, Dakar, Senegal

[2]Electronics, Informatics, Telecommunications, and Renewable Energy Laboratory,
Faculty of Applied Sciences and Technology, Gaston Berger University, Saint-Louis, Senegal

Abstract: The aim of this work is to present a theoretical study of a vertical junction silicon solar cell under monochromatic illumination. By solving the continuity equation and using a one-dimensional model in frequency modulation, we derive the analytical expressions of both excess minority carrier density and photovoltage. Based on these expressions, the solar cell capacitance was calculated; we then exhibited the effects of both illumination wavelength and incidence angle on the solar cell capacitance.

Key words: Vertical junction, capacitance, frequency modulation

1. Introduction

The performance of solar cells is often limited by the recombination of photogenerated carriers before they reach the junction and cross it to take part in the photocurrent. Thus, the knowledge of certain parameters and the control of technological processes are of utmost importance [1,2] when designing these optoelectronic devices.

Many characterization methods [3] in the steady state [4,5], as well as the transient state [6,7] or frequency modulation [8,9], were developed for the determination of one or several parameters of the solar cell.

In this work, we first derive the excess minority carrier density and the photovoltage across the junction; these expressions then lead to the solar cell capacitance. The aim of this study is to show the effects of the illumination incidence angle and wavelength on the solar cell's capacitance; for that purpose, this capacitance is studied for various incidence angles and illumination wavelengths in frequency modulation. The Bode diagram of the solar cell capacitance exhibited a cut-off frequency, and this study also show how this cut-off frequency depends on both incidence angle and illumination wavelength.

2. Theory

This study is based on a vertical junction silicon solar cell, presented in Figure 1, with the following assumptions:

- The space charge region and the emitter thicknesses are very small compared to that of the base; their contributions are then neglected so that only the contribution of the base is taken into account [10].
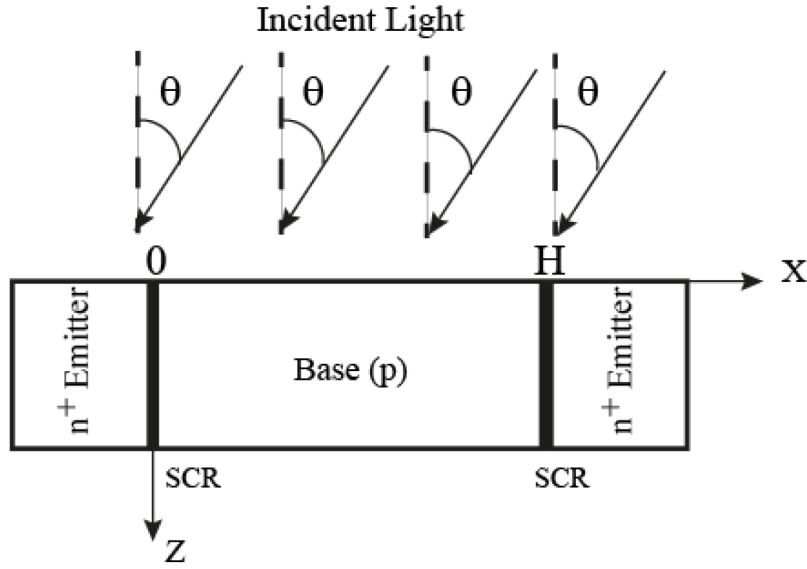
---

*Correspondence: barrofabe@gmail.com

Figure 1. Vertical junction unit cell.

- The emitter and the base regions are quasineutral [11]; there is no internal electric field without the space charge region.

- The electric and optical properties are identical at any point in the base; this enables us to use the Cartesian coordinates. We also took into account the reflection on the silicon material.

- The temperature effect on the performance of the photovoltaic cell is not taken into account.

- The excitation is done with a monochromatic frequency modulated light with wavelength λ. The incident photon flux $\varphi(\lambda)$ is taken for the AM 1.5 solar spectrum [12,13]. This case is characteristic of the whole terrestrial applications independently of the processing site. Indeed, the solar radiation corresponds roughly to that of a black body at 6000 K; while crossing the various layers of the atmosphere, certain wavelengths are attenuated by components of the atmosphere such as ozone (absorption of UV rays in the neighborhood of 400 nm) or water vapor (absorption of the infrared wavelengths around 800–900 nm).

Taking into account the generation, recombination, and diffusion phenomena in the base, the equation governing the variation of the minority carrier density δ(x,θ,z,t) under modulation frequency [7,8] is:

$$D(\omega) \cdot \frac{\partial^2 \delta\left(x, \theta, z, t\right)}{\partial x^2} - \frac{\delta\left(x, \theta, z, t\right)}{\tau} = -G(z, \theta, t) + \frac{\partial \delta\left(x, \theta, z, t\right)}{\partial t}. \tag{1}$$

$D(\omega)$ and τ are respectively the excess minority carrier diffusion constant and lifetime, ω is the angular frequency, x is the base depth along the x axis, θ is the incidence angle, and z is the base depth according to the vertical axis. δ(x,θ,z,t) is the excess minority carrier density and G(z,θ,t) is the carrier generation rate.

The excess minority carrier density can be written as:

$$\delta\left(x, t\right) = \delta\left(x\right) \exp\left(-j\omega t\right). \tag{2}$$

The carrier generation rate is given by [4,8,14]:

$$G\left(z, \theta, \lambda, t\right) = g\left(z, \theta, \lambda\right) \exp\left(-j\omega t\right), \tag{3}$$

where the spatial part is given by:

$$g\left(z, \theta, \lambda\right) = \alpha(\lambda)(1 - R(\lambda)) \cdot \varphi(\lambda) \cdot \exp(-\alpha(\lambda) \cdot z) \cdot \cos(\theta). \tag{4}$$

Here, λ is the illumination wavelength, $\alpha(\lambda)$ and $R(\lambda)$ are respectively the absorption and reflection coefficients, t is the time, and $j^2 = -1$.

If we replace Eq. (2) into Eq. (1), the temporary part $\exp(-j\omega t)$ is eliminated and we obtain:

$$\frac{\partial^2 \delta\left(x\right)}{\partial x^2} - \frac{\delta\left(x, \theta, t\right)}{L(\omega)^2} = -\frac{g(z, \theta)}{D(\omega)}, \tag{5}$$

where $L(\omega)$ is the minority carrier diffusion length.

The solution of Eq. (5) is:

$$\delta\left(x, \omega, \theta, z, \lambda\right) = A \cosh\left(\frac{x}{L(\omega)}\right) + B \sinh\left(\frac{x}{L(\omega)}\right) + \frac{L(\omega)^2}{D(\omega)} \cdot \alpha(\lambda)(1 - R(\lambda)) \cdot \varphi(\lambda) \cdot \exp(\alpha(\lambda) \cdot z) \cdot \cos(\theta) \qquad . \tag{6}$$

Coefficients A and B are determined with the following boundary conditions [4] at the junction (x = 0):

$$D(\omega) \cdot \left.\frac{\partial \delta\left(x, \omega, \theta, z, \lambda\right)}{\partial x}\right|_{x=0} = Sf \cdot \delta\left(x, \omega, \theta, z, \lambda\right)|_{x=0}. \tag{7}$$

Sf is the junction recombination velocity traducing carrier flow through the junction.

Meanwhile, at the middle of the base (x = H/2):

$$D(\omega) \cdot \left.\frac{\partial \delta\left(x, \omega, \theta, z, \lambda\right)}{\partial x}\right|_{x=\frac{H}{2}} = 0. \tag{8}$$

H is the base depth.

Based on the excess minority carrier density, we can determine the photovoltage across the junction.

According to Boltzmann's relation, the photovoltage is obtained by following the expression [3,15]:

$$V\left(\omega, \theta, z, \lambda\right) = V_T \cdot \ln\left[1 + \frac{Nb}{n_0^2} \cdot \delta\left(0, \omega, \theta, z, \lambda\right)\right], \tag{9}$$

where V_T is the thermal voltage, Nb the base doping density, n_0 the intrinsic carrier density, and q the elementary charge.

Based on minority carrier density and photovoltage, we can determinate the capacitance of the solar cell. This capacitance is mainly due to the fixed ionized charge (dark capacitance) at the junction boundaries and the diffusion process (diffusion capacitance) [15–17]. The solar cell's capacitance can be defined by :

$$C\left(\omega, \theta, z, \lambda\right) = \frac{dQ\left(\omega, \theta, z, \lambda\right)}{dV\left(\omega, \theta, z, \lambda\right)}, \tag{10}$$

with

$$Q\left(\omega, \theta, z, \lambda\right) = q \,\delta(x, \omega, \theta, z, \lambda)|_{x=0}. \tag{11}$$

Given the photovoltage expression, Eq. (10) can be rewritten as:

$$C\left(\omega, \theta, z, \lambda\right) = \frac{q}{V_T} \cdot \left(\frac{n_i^2}{Nb} + \delta\left(0, \omega, \theta, z, \lambda\right)\right).$$ (12)

Under illumination, the diffusion capacitance predominates. Based on all the previous expressions and some computation, we obtain the behavior of the solar cell capacitance as presented in the next section.

3. Results and discussion

3.1. Incidence angle effect

We present the capacitance of the solar cell versus modulation frequency (semilogarithmic scale) for various incidence angles (Figure 2).

Figure 2 shows that the solar cell's capacitance remains practically constant while the modulation frequency is below a certain threshold value ω_c; above this threshold, the capacitance decreases markedly.

Effectively, below ω_c the solar cell is in a quasisteady state such that minority carriers are not very sensitive to the modulation frequency. Above ω_c, carriers cannot diffuse properly because of the modulation frequency becoming so much higher than the carriers' relaxation time; this leads to a decrease of the diffusion capacitance, which is the major component of the illuminated solar cell capacitance, as observed. This threshold frequency ω_c is also called the cut-off frequency.

When the incidence angle increases, the incident photon flux penetrating the solar cell decreases due to the reflection coefficient; this leads to a decrease of excess carrier concentration in the base and thus a decrease of the capacitance for a given operating point.

We present in Figure 3 the determination of the cut-off angular frequency ω_c [17] for a given incidence angle.
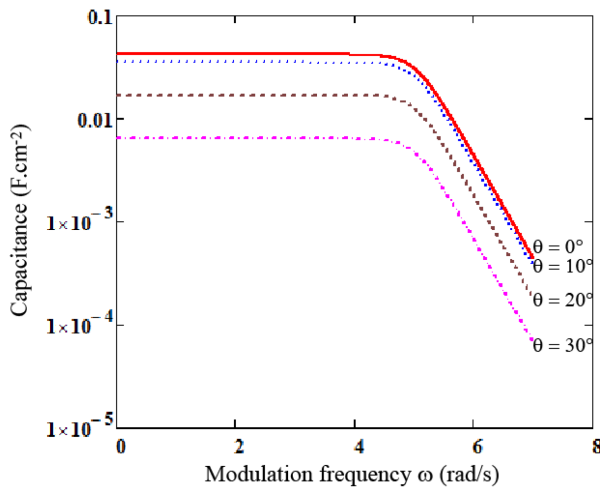

Figure 2. Capacitance versus modulation frequency (log scale) for various incidence angles. Sf $= 3 \times 10^{-3}$ cm/s, H $= 0.03$ cm, Lo $= 0.02$ cm, Do $= 26$ cm^2/s, $\lambda = 600$ nm, z $= 0.0001$ cm.
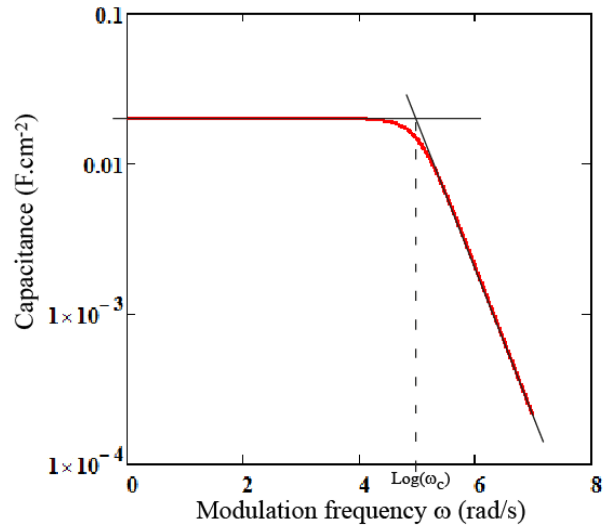
Figure 3. Cut-off frequency determination (logarithmic scale). $\theta = 48.2°$, Sf $= 3 \times 10^{-3}$ cm/s, H $= 0.03$ cm, Lo $= 0.02$ cm, Do $= 26$ cm^2, $\lambda = 600$ nm, z $= 0.0001$ cm.

The cut-off frequency ω_c ($\omega_c = 5.8 \times 10^5$ rad/s; Figure 3) corresponds to the intercept point of the 2 linear parts of the capacitance curve.

Based on Figure 3, we determined the cut-off frequency for various incidence angles; Figure 4 then illustrates the dependence of the cut-off frequency on the incidence angle.

One can see that the cut-off frequency effectively increases with increasing incidence angle, as we observed previously.

The next subsection presents the effect of the illumination wavelength on the solar cell capacitance.

3.2. Wavelength effect

We want to illustrate the effect of illumination wavelength on the behavior of the solar cell capacitance.

Figure 5 shows the solar cell capacitance versus modulation frequency for illumination wavelengths in the range of [400 nm; 460 nm].
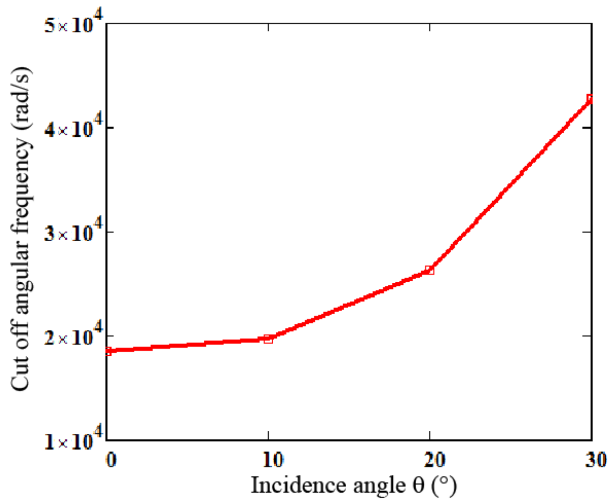

Figure 4. Cut-off frequency for various incidence angles. Sf $= 3 \times 10^{-3}$ cm/s, H $= 0.03$ cm, Lo $= 0.02$ cm, Do $= 26$ cm^2/s, $\lambda = 600$ nm, z $= 0.0001$ cm.
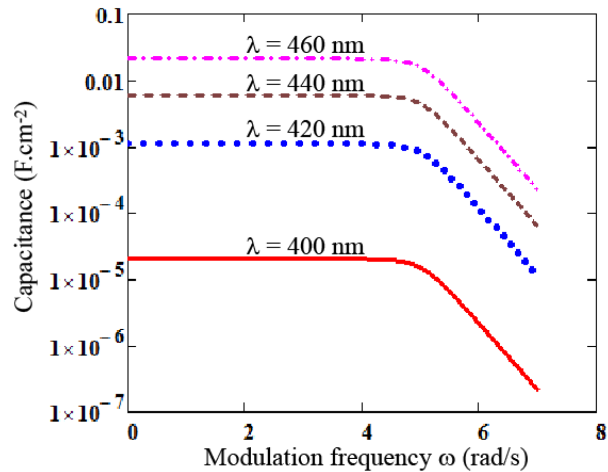
Figure 5. Solar cell capacitance versus modulation frequency (logarithmic scale) for lower illumination wavelength. H $= 0.03$ cm, Lo $= 0.02$ cm, Do $= 26$ cm^2/s, $\omega = 10^3$ rad/s, $\theta = 48.2°$, z $= 0.0001$ cm.

We observe that solar cell capacitance still behaves as described in Figure 2 with modulation frequency. When the wavelength increases from 400 to 460 nm, the increase of the wavelength in this range effectively leads to an increase of the excess minority carrier density for a given operating point so that the capacitance also increases. The cut-off frequency is left-shifted for a lower illumination wavelength.

Figure 6 illustrates the behavior of the capacitance for illumination wavelengths in the range of [780 nm; 980 nm].

One can see that this behavior is inverted compared to that of Figure 5. For this wavelength range, the excess minority carrier density decreases and the capacitance also decreases; contrary to Figure 5, the cut-off frequency is now right-shifted.

We present in Figure 7 the evolution of the cut-off angular frequency versus illumination wavelength.
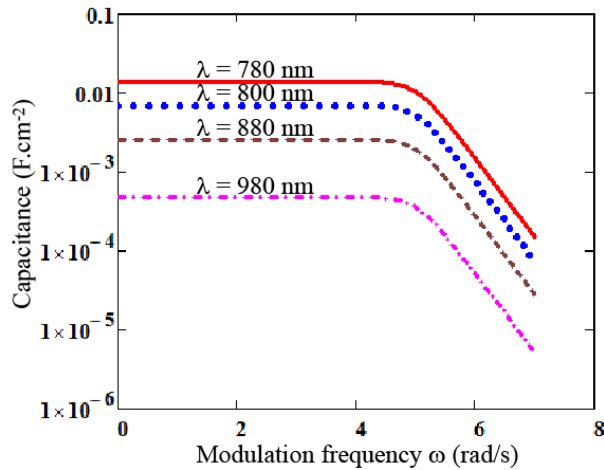
Figure 6. Solar cell capacitance versus modulation frequency (logarithmic scale) for higher illumination wavelength. H = 0.03 cm, Lo = 0.02 cm, Do = 26 cm^2/s, ω = 10^3 rad/s, θ = 48.2°, z = 0.0001 cm.
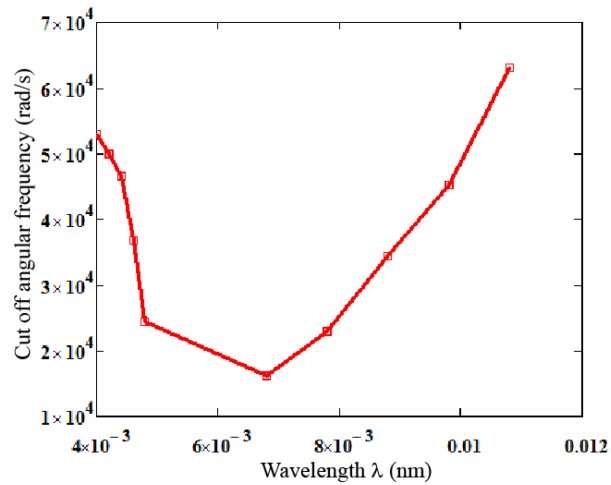
Figure 7. Cut-off frequency versus illumination wavelength. H = 0.03 cm, Lo = 0.02 cm, Do = 26 cm^2/s, θ = 48.2°, z = 0.0001 cm.

One can see that the cut-off frequency decreases for short wavelengths, contrary to long wavelengths. Given that for short wavelengths the carrier generation takes place near the junction, the associated time constant will increase, and, according to the relation $\omega c = 2\pi/\tau$ [18], the cut-off frequency will then decrease as observed above; this behavior is inverted for long wavelengths.

4. Conclusion

A theoretical study of a vertical junction solar cell has been presented. Based on the excess minority carriers' density and the photovoltage, the solar cell capacitance was calculated and the cut-off frequency was then deduced. This capacitance (resp. cut-off frequency) was then studied for various incidence angle and illumination wavelengths, and we showed that the solar cell's capacitance and cut-off frequency strongly depend on both incidence angle and illumination wavelength. For the considered range of incidence angles, the capacitance (resp. cut-off frequency) decreases (resp. increases) with increasing incidence angle; for short wavelengths, the capacitance (resp. cut-off frequency) increases (resp. decreases), but this behavior is inverted for long wavelengths.

References

[1] Miles, R. W.; Hynes, K. M.; Forbes, I. *Prog. Cryst. Growth Ch.* **2005,** *51*, 1–42.

[2] Glunz, J. W. *Advances in Opto-Electronics* **2007**, *2007*, 97370.

[3] Sze, S. M.; Kwok, K. Ng. *Physics of Semiconductors Devices*; Wiley: New York, NY, USA, 2007.

[4] Diallo, H. L.; Wereme, A.; Maiga, A. S.; Sissoko, G. *Eur. Phys. J. Appl. Phys.* **2008**, *42*, 203–211.

[5] Mbodji, S.; Mbow, B.; Barro, F. I.; Sissoko, G. *Turk. J. Phys.* **2011**, *35*, 281–291.

[6] Barro, F. I.; Maiga, A. S.; Wereme, A.; Sissoko, G. *Phys. Chem. News* **2010**, *56*, 76–84 .

[7] Gaye, I.; Sam, R.; Seré, A. D.; Barro, I. F.; Ould El Moujtaba, M. A.; Mané, R.; Sissoko, G. *International Journal of Emerging Trends and Technology in Computer Science* **2012,** *1*, 210–214.

[8] Dieng, A.; Zerbo, I.; Wade, M.; Maiga, A. S.; Sissoko, G. *Semicond. Sci. Technol.* **2011**, *26*, 095023.

[9] Thiam, A.; Zoungrana, M.; Ly Diallo, H.; Diao, A.; Thiam, N.; Gueye, S.; Deme, M. M.; Sarr, M.; Sissoko, G. *Res. J. Appl. Sci. Eng. Technol.* **2012**, *5*, 1123–1128.

[10] Sissoko, G.; Nanéma, E.; Corréa, A; Adj, M.; Ndiaye, A. L.; Diarra, M. N. *Renew. Energ.* **1998,** *3*, 1856–1859.

[11] Mathieu, H.; Fanet, H. *Physique des semiconducteurs et des composants électroniques*, 6th ed.; Dunod: Paris, France, 2009.

[12] Green, M. A.; Emery, K.; Hishikawa, Y.; Warta, W. *Prog. Photovolt. Res. Appl.* **2010**, *18*, 144–150.

[13] Green, M. A. *Sol. Energ. Mat. Sol. C.* **2008**, *92*, 1305–1310.

[14] Diallo, H. L.; Dieng B.; Ly, I.; Dione, M. M.; Ndiaye, M.; Lemrabott, O. H.; Bako, Z. N.; Wereme, A.; Sissoko, G. *Res. J. Appl. Sci. Eng. Technol.* **2012**, *4*, 2626–2631.

[15] Hu, C. C. *Modern Semiconductor Devices for Integrated Circuits*; Pearson/Prentice Hall: Upper Saddle River, NJ, USA, 2010.

[16] Boer, K. W. *Introduction to Space Charge Effects in Semiconductors*; Springer-Verlag: Berlin, Germany, 2010.

[17] Barsoukov, E.; Macdonald, J. R. *Impedance Spectroscopy: Theory, Experiment and Applications*; Wiley: New York, NY, USA, 2005.

[18] Kosyachenko, L. A. *Solar Cells – Dye-Sensitized Devices*; InTech: Rijeka, Croatia, 2011.